CLASSIFYING INDONESIAN PLANTATION AND NATURAL FOREST COVER AND MEASURING CHANGES WITH C- AND L-BAND SAR DATA

Xichao Dong [(1)(2)], Shaun Quegan [(1)], Yumiko Uryu [(3)] Tao Zeng[(2)]

[(1)] CTCD, University of Sheffield, Hicks Building, Sheffield S3 7RH, United Kingdom, Email:s.quegan@shef.ac.uk
[(2)] Beijing Institute of Technology, Beijing 100081, China, Email:maxwill551@gmail.com
[(3)] World Wildlife Fund, 1250 24th Street, NW, WA, DC 20037, USA, Email: yumuryu@yahoo.com

ABSTRACT

Tropical coverage by Envisat is sparse in space and time and has limited value for monitoring deforestation. The only available APG multi-temporal dataset over Riau province, Indonesia (9 images in a single year), is used to distinguish and monitor tropical plantations and their dynamics and is compared with L-band PALSAR data. For Envisat APG data, both VV and VH are important in discriminating different types of forest cover, while at L-band most of the relevant information is in the cross-polarised channel. Whether the underlying soil is peat or non-peat in acacia plantations has important effects on backscatter and classification. Supervised classification of the C-band data gave overall accuracies of 86.2% and kappa coefficient of 0.78 by comparison with land cover maps derived from optical data. Classifications from separate phases in the C-band time series allow the changes occurring in acacia plantations due to management to be tracked.

1. INTRODUCTION

During the first decade of the 21st century, deforestation rates in tropical countries are reported to have declined significantly relative to the 1990s [1], but tropical deforestation still has a significant impact on the planetary carbon balance, leading not only to loss of the ability to take up carbon but also additional carbon emissions from biomass burning or decay arising from the clearing process. The deforestation process ranges from large-scale felling in order to establish plantations, agriculture and pasture, to small-scale clearance for shifting agriculture [2]. These conversions can bring major commercial profits for companies and job opportunities for local people.

In Indonesia, Riau Province had the highest deforestation rate at an annual average of up to 4.8% from 1985 to 2008 and may have contributed to around 60% to Sumatra's total emissions from natural forest loss [3]. Most of the cleared land is being replaced by rapidly expanding commercial oil palm and acacia plantations: Riau is the largest producer of palm oil in Indonesia, with up to 24% of the total national production [4], and also possesses high capacity pulp industry mills, which generate more than two thirds of Indonesia's pulp and paper production [5]. Increasingly, these plantations are being located on peatland, which stores large amounts of carbon. This causes sustained greenhouse gas emissions that arise not only during forest clearance but from continual soil oxidation during the plantation rotation cycle, especially for short rotation acacia plantations [6]. Hence, although good management of established plantations or other land use areas can reduce the pressure to clear natural forest, peatlands will still yield significant carbon emissions. Systematic monitoring of tropical plantations will help to estimate and manage their magnitude.

Remote sensing of forest changes using optical, short-wave or near-infrared reflectance and thermal spectra is now well established [7, 8]. However, there are large gaps in Indonesian data due to cloud cover and haze, which affect the production of annual land cover maps, although large area maps of forest cover loss over a multi-year interval are feasible by combining cloud-free Landsat 7 time series [9]. The higher observation frequency of MODIS provides more frequent cloud-free imagery [10], but these data are inadequate for accurately estimating deforestation since much deforestation occurs at sub-pixel scale at the coarser spatial resolution of MODIS [11-13].

Synthetic Aperture Radar (SAR) is an alternative technology for monitoring tropical forest, with the major advantage that it can provide images under all weather conditions, whenever there is a satellite pass. Furthermore, radar is more sensitive to ground conditions and vegetation structure, and more physically related to the biomass than other remote sensing methods [14, 15]. However, the use of radar for this purpose has been hampered by the lack of access to data and the immaturity of methods. The five-year archive of systematic global forest coverage by the ALOS-PALSAR radar until its failure in April 2011 has allowed methods to be developed for L-band data [16], but these have not yet been extensively tested. C-band is much less developed, not least because ENVISAT ASAR has sparse and patchy spatial and temporal coverage over tropical areas. However, this situation will change dramatically in late 2013 when the launch of the first C-band Sentinel-1 satellite will guarantee open access data with a revisit time of 12 days at the equator and systematic global coverage [17]. The JAXA L-band ALOS-2 mission is also expected to be launched around the same time, and to continue the policy of global forest data acquisition established for ALOS-1, although there are concerns that JAXA's pricing policy may hinder use of these data as part of a global tropical

Proc. 'ESA Living Planet Symposium 2013', Edinburgh, UK
9–13 September 2013 (ESA SP-722, December 2013)

forest monitoring system. Nonetheless, the availability of simultaneous L- and C-band data opens up exciting new prospects for tropical forest monitoring and management.

Our original plan was to analyse joint use of C- and L-band data to monitor tropical deforestation, but the limited available Envisat datasets for Riau did not contain such events. Instead, this paper explores the use of C- and L-band SAR data to monitor tropical plantations and their dynamics. After describing the ground and satellite datasets, the behaviour of radar backscatter from tropical forest and plantations is investigated for both C- and L-band data. Supervised classification is then performed to produce thematic maps, which are tested by comparison with land cover maps derived from optical data. Finally, the classification results from separate phases in the C-band time series are used to track the changes occurring in acacia plantations due to management.

2. STUDY SITES AND DATA

The study site lies in Riau province, Sumatra, Indonesia, which has extensive natural forest cover but with much clearance for commercial acacia and oil palm plantations. Most of the deforestation is traceable in L-band data. However, as for most of the tropics, coverage by ASAR is limited and dual polarisation data are available only from late 2010 to late 2011. During this period, though ASAR provides coverage of ~100x100 km^2, little deforestation occurred in the area due to limited issues of clearance licences and pressures from the social community. Few changes were also seen in the oil palm plantations, as the oil production process does not involve much clearance or replanting. In contrast, acacia is harvested every 4-6 years to provide wood pulp, followed by replanting to begin the next rotation cycle. Hence acacia plantations exhibit regular periodic changes, with stand ages covering the range from planting to harvest, and then back to planting. Both harvest and regrowth of acacia occurred in the study period, and is traceable in the SAR data.

Fig. 1 shows the locations of the study site and the available radar data. On the left, the background image is derived from an ALOS PALSAR Orthorectified Mosaic Product, which is a 50m reference dataset created under the ALOS Kyoto and Carbon Initiative (K&C) from ALOS PALSAR fine beam dual polarisation (FBD) acquisitions in 2009 [18]. The mosaic product is geometrically rectified using a SRTM 90m Digital Elevation Model and projected into the WGS-1984 coordinate system.

The red rectangle indicates the coverage by ASAR Alternative Polarization Geocoded Ellipsoid Corrected (APG) data. These consist of nine VV- and VH-polarized image pairs with spatial resolution of around 30m in range and 30m in azimuth and 12.5m pixel spacing acquired from track 377 over the period November 2010 to October 2011. These multi-look products have an equivalent number of looks (ENL) greater than 1.8 and have been relatively calibrated, geocoded and resampled to a map projection [19]. There is little temporal overlap between the K&C mosaics and the C-band data, since ALOS failed in April 2011.

The reference map shown on the right top of Fig. 1 was produced for the World Wildlife Fund (WWF) using Landsat images. It is mainly based on the December 2011 image from row 126 and path 60, although images from different dates were used to mitigate cloud and haze. Three types of tree cover are identified (oil palm and acacia plantations and natural forest), while other types of land cover, including cleared area, are marked as unclassified. Note that in our analysis cleared areas are identified by comparing the Landsat-7 image and the SAR images (as shown in Fig. 3) visually. In the Landsat image, exposed soil appears purple and is easily discriminated from water bodies and vegetation. The corresponding regions can be used to select training areas in SAR images. Fig. 1 (bottom right) shows the spatial distribution of peat soils within the ASAR scene according to WWF datasets. Acacia and oil palm plantations occur on both peat and non-peat soils, but natural forest and cleared areas only on peat soils. Three regions of interest, A, B and C, are marked and are inspected in the backscatter analysis: A is natural forest on a peat dome, while B and C are both acacia plantations but in different growing phases.

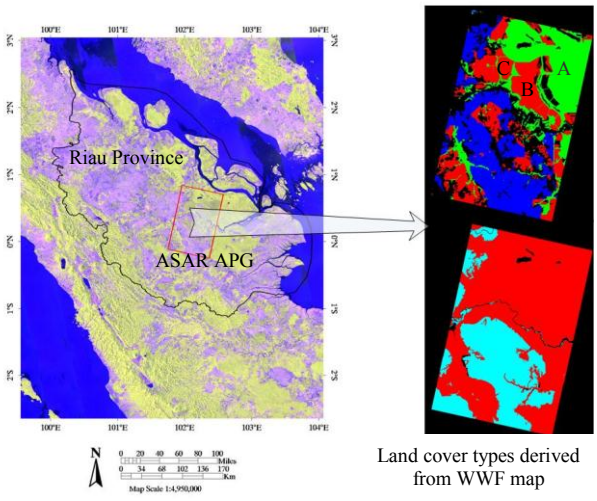

Figure 1 Left: Geographical locations and SAR datasets from ESA Envisat ASAR (© European Space Agency) and JAXA ALOS PALSAR KC 50m mosaics (© JAXA, METI). The background image is derived as an RGB composite from the ALOS mosaic for 2009, with red, green and blue corresponding to HH, HV and HH/HV respectively. Top right: Land cover types in the ASAR APG scene derived from WWF map; green: natural forest; red: acacia; blue: oil palm; black: unclassified. Bottom right: distribution of peat soil in the ASAR scene; red: peat; cyan: non-peat.

The acquisition dates of the satellite datasets are shown in Fig. 2. In order to measure changes, the nine C-band images are divided into three subsets, viz.: 1) November & December 2010 and January 2011; 2) March, April & May 2011; 3) June, July & October 2011, which we will refer to as winter, spring and summer respectively, despite the lack of any strong seasonality at these latitudes. The acquisition dates of the images in the third subset are closest to the date of the Landsat image on which the WWF land cover map is mainly based, so this subset is used for accuracy assessment. The earlier subsets are used to monitor plantation dynamics.

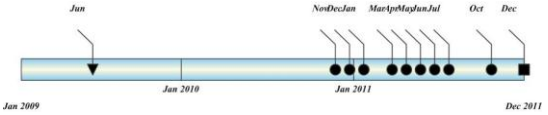

Figure 2 Acquisition dates of ASAR APG (circles), ALOS PALSAR 50m mosaic (triangle) and Landsat 7 (square) datasets.

3. METHOD

3.1. SAR Image Processing

Absolute calibration and registration of the ASAR APG time series was performed using GAMMA software, and the images were speckle-reduced in a two-stage approach involving multi-channel filtering [20] followed by mean filtering with 23×23 window size [16].

PALSAR mosaic tiles were downloaded from JAXA's website [21] and mosaiced by georeferencing in IDL/ENVI to obtain full coverage of Sumatra. The mosaics were then masked by the footprint of the ASAR scene and the amplitude DN values were converted to radar backscattering coefficient (σ^0) in dB using the relation [22]:

$$\sigma^0 = 10 \times \log_{10} \left\langle \mathrm{DN}^2 \right\rangle + \mathrm{CF} \qquad (1)$$

where CF is a calibration constant equal to -83 dB.

3.2. Supervised Classification and Verification

The filtering process ideally causes the pixel values in a uniform distributed target to obey a Gamma distribution [23] with a large ENL, which is therefore approximately Gaussian and suitable as input to a maximum likelihood (ML) classifier. Training data for each land cover category were selected on the basis of the WWF maps and used to drive ML classification on each APG subset, leading to three thematic maps. The accuracy of the classifications was assessed in terms of overall accuracy and kappa coefficient derived from the confusion matrix, treating the WWF map as reference data.

4. RESULTS

4.1. Backscatter Analysis

Landsat 7, ASAR C-band and PALSAR L-band images of the study area are given in Fig. 3 as colour composites. The ASAR image is from October 2011, with red and green corresponding to the VV and VH channels respectively and blue to the VV/VH ratio. The RGB composite for the 2009 PALSAR L-band mosaic shows the HH and HV channels in red and green and the HH/HV ratio in blue (note: for convenience, below we use "channel" to include the ratio data). The Landsat image was acquired in December 2011 and its RGB composition channels are bands 50, 40 and 30. The panel on the right is an enlargement of region B in the APG and PALSAR data displaying more details of an acacia plantation. Much more structure is visible at L-band than at C-band (notably linear features associated with tree spacing) because of the greater penetration and sensitivity to the vegetation structure at L-band. This may aid visual interpretation but is likely to yield errors in automatic classification.

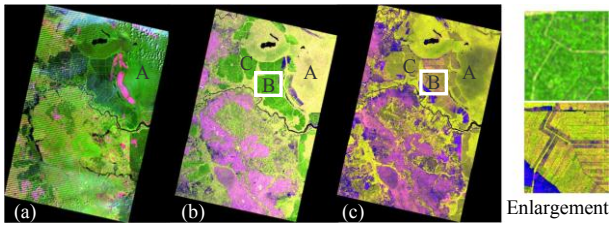

Figure 3 RGB composites of the study area. (a) Landsat-7 from December 2011: RGB correspond to bands 50, 40 and 30 respectively; (b) ASAR APG from October 2011: RGB correspond to VV, VH and VV/VH respectively; (c) PALSAR 50m mosaic, data acquired in 2009: RGB correspond to HH, HV and HH/HV respectively. The right panels show enlargements of region B of ASAR APG (top) and PALSAR 50m mosaic (bottom) separately.

The colours in Fig. 3 indicate the different scattering behaviours of various land cover types, and, by comparison with Fig. 1 (right), suggest the potential for separating natural forest, acacia and oil palm plantations. As already mentioned, acacia and oil palm plantations occur on both peat and non-peat soils. While oil palm exhibits similar backscatter on both types of soil, there are big differences for acacia as illustrated by the histograms of the ASAR and PALSAR co-polarised, cross-polarised and polarisation ratio values for natural forest, acacia on peat and non-peat soils, oil palm and cleared areas shown in Fig. 4 (these histograms use all available pixels within each land cover). Hence, classification and accuracy assessment is performed on peat and non-peat soils separately.

For ASAR, natural forest has the greatest backscatter in both the VH and VV channels, particularly VH. Acacia plantations on peat and non-peat soils have similar VH behaviour, but are quite different in VV, with plantations on peat soils giving the lowest VV backscatter amongst all classes. Oil palm gives the second largest backscatter in VV, but, along with

cleared areas, the lowest VH backscatter. By contrast, the VV backscatter from cleared areas is greater than from acacia plantations on peat soils and comparable to that from acacia on non-peat.

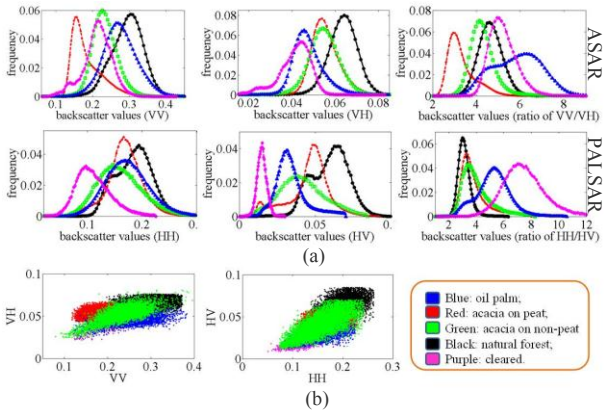

Figure 4 (a) Histograms of values using all available pixels for (top) ASAR VV, VH and VV/VH; (bottom) PALSAR HH, HV and HH/HV for five classes: natural forest (black), acacia on peat (red), acacia on non-peat (green); oil palm (blue) and cleared area (purple). (b) 2D distribution of random samples of the five classes with pixels lying within the 5% cut-off of the histogram tails in both co- and cross-polarised channels.

The L-band HH channel exhibits much less discrimination between different land covers than the C-band co-polarised channel, and HV is much more important for separating the classes, with clear backscatter differences between natural forest, acacia plantations on peat, oil palm and cleared areas. However, there are large overlaps between the distribution for acacia plantations on non-peat soils and those of all other cover types except cleared areas. Cleared areas have the lowest backscatter in both the HH and HV channels. In the HV channel, natural forest has the highest backscatter but a bimodal distribution, in which the lower peak corresponds to a peat dome where the backscatter is lower than for the surrounding natural forest and is comparable to the values for acacia plantations on peat soils. This hinders the separation of natural forest from other land covers, such as acacia plantations, if only L-band is used. The histograms for acacia plantations have long tails because they are in various growth phases, as can be seen in regions B and C in Fig. 3, unlike for ASAR. Hence ALOS PALSAR mosaics can provide more information on vegetation status but this complicates automatic classification of natural forest and plantations.

Significant overlaps between classes, as seen in the individual channels, also occur in their 2-D distributions (Fig. 4(b), which shows the histogram of cross-polarised against co-polarised data for both C- and L-band), which will induce classification errors.

While some of the observed behaviour would be expected physically, such as the large cross-polarised values due to volume scattering from natural forest, other aspects of the data, such as the very low values of VV backscatter for acacia on peat soils, cannot as yet be readily explained.

4.2. Classification

The above backscatter analysis provides information on factors affecting classification using the C- and L-band data. For example, knowing the spatial distribution of peat and non-peat soils is clearly essential. Also, all three channels have discriminating capability at C-band, while for L-band the HH channel contributes little except through its partial separation of cleared areas. What is unclear is whether there is any gain in using all three channels, or whether the ratio data are redundant if the co- and cross-polarised channels are used (clearly, no extra information is supplied by including the ratio, but it may prove more effective within a given classification algorithm).

Classification was performed on four separate sets of data: the PALSAR mosaic and the three subsets of ASAR APGs. The PALSAR set consists of the HH, HV and HH/HV ALOS PALSAR images derived from the K&C mosaics for 2009. For ASAR APG, each set contains the VV, VH and VV/VH images for three months (the winter, spring and summer subsets for 2010-2011 described in Section 2), so there are 9 images in each set. Water bodies are masked out because they become blurred in the filtering steps and induce misclassifications. The ASAR APGs are pre-processed by a multi-channel filtering followed by spatial averaging over a 23×23 pixel window [16]. The PALSAR mosaics are used directly because they are already speckle-reduced by JAXA. The training data is selected using the WWF maps and identification of cleared areas is refined using the Landsat image.

ML is applied to each APG data subset, and to remove isolated small regions, for both PALSAR mosaic and ASAR APGs, regions smaller than 9 pixels are reclassified to the class of the surrounding area. Since the acquisition dates of the images in the winter 2011 ASAR APG subset are closest to the date of the Landsat image of most importance in producing the WWF map, this subset is used to assess classification accuracy.

The analysis in Section 4.1 suggested that some classes were better discriminated using the VV/VH ratio than in either VV or VH. Hence classification was carried out using four different combinations of the polarized channels: VV and VH, VV and VV/VH, VH and VV/VH, and all three channels. On peat soils, although the VH and VV/VH pair gives marginally better accuracy than the other combinations in terms of overall accuracy and kappa coefficient (see Tab. 1), the improvement is marginal, so we base the results below on the combination of VV and VH, as this is computationally more efficient.

Table 1 Overall accuracy (%) and kappa coefficient of classification on peat soils using different combinations of the VV, VH and VV/VH channels

	VV & VH	VV & VV/VH	VH & VV/VH	VV, VH & VV/VH
Overall accuracy	85.9	84.3	86.2	85.2
Kappa coefficient	0.77	0.74	0.78	0.76

Fig. 5 shows the classifications based on PALSAR 2009 mosaics and the ASAR summer 2011 subset. For PALSAR, natural forest in region A is misclassified as acacia, for reasons clear from the backscatter analysis and histograms. ASAR shows better visual similarity with the WWF maps (see Fig. 1 right).

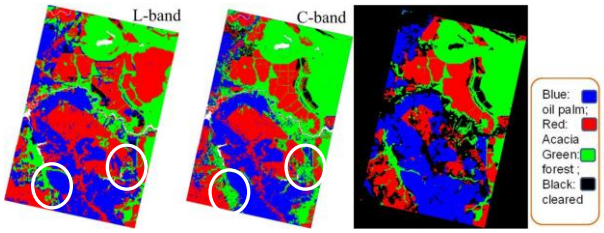

Figure 5 Classifications for (left) PALSAR 2009 L-band mosaic and (middle) APG C-band summer 2011 subset. Red: acacia on peat; yellow: acacia on non-peat; blue: oil palm; green: natural forest; black: cleared. The WWF classification is shown on the right.

Tab. 2 lists the confusion matrices for APG classifications on peat and non-peat soils separately (natural forest occurs only on peat soils in the region covered by these images). On peat soils, many acacia and oil palm plantations are misclassified as natural forest. Examples include the two circled areas in Fig. 5 (middle): the left and right circled areas are in fact acacia and oil palm respectively, not natural forest. Possible factors are that the oil palm plantations here are younger than elsewhere (according to the WWF database, oil palm here was planted after 2005 and the others were planted before 2000) and the acacia is in a hilly area where terrain variations affect the backscatter. These two areas are correctly classified in L-band. Hence, though L-band gives serious errors in the natural forest on the peat dome, it can help to correct the C-band classifications, although how to make correct decisions when there are inconsistencies between C- and L-band classifications is an unresolved issue and we have yet to carry out classification using both data types together.

For non-peat soils, 22.7% of the oil palm area is misclassified as acacia because of the significant overlaps of the data (Fig. 4) and the weightings imposed in the ML classification.

Table 2 Confusion matrices for the APG C-band summer 2011 subset (values given as %). Columns correspond to ML classification and rows to map data.

(a) Confusion matrix for peat soils

Class	Acacia on peat	Natural forest	Oil palm
Acacia on peat	73.6	0.60	0.24
Natural forest	22.0	96.8	17.8
Oil palm	4.30	2.61	82.0

(b) Confusion matrix for non-peat soils

Class	Acacia on non-peat	Oil palm
Acacia on non-peat	96.3	22.7
Oil palm	3.70	77.4

4.3. Dynamics of Acacia Plantations

Section 4.2 has shown that many of the errors in classifying acacia plantations in APG data arise from their harvest and replanting cycle. This suggests that time series of C-band data can be used to monitor such changes. To assess this, classifications for the three temporal subsets are used to build clearance (Fig. 6a) and replanting (Fig. 6b) maps for acacia plantations. In Fig. 6a, black shows harvest in 2010 while cyan and magenta show harvest in spring and summer 2011. Replanting is carried out soon after harvest because cleared areas are classified as vegetated in the next subset, as shown in Fig. 6b. Black is cleared areas that have not yet been replanted, yellow and magenta show regrowth in early and mid-2011. If acquisitions are provided frequently enough, e.g. by Sentinel-1, such data can be used to track plantation status and monitor the activity of pulp companies. Although the available APG has not allowed this to be directly assessed, such a system is also likely be invaluable for monitoring illegal clearance of natural forest.

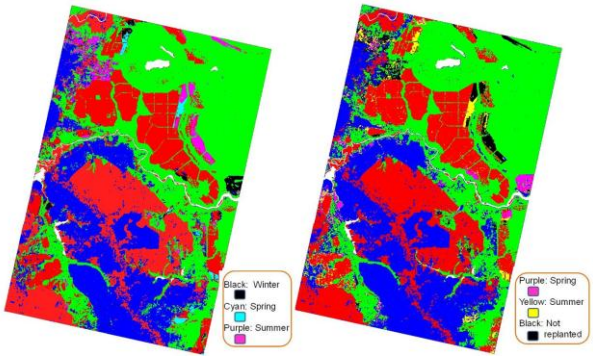

Figure 6 Dynamics of clearance (left) and regrowth (right) of acacia plantations derived from ASAR APG time series.

5. CONCLUSIONS

This paper analyses C- and L-band SAR backscatter for tropical forest and plantations and the use of C–band time series to track plantation dynamics. Our main conclusions are:

a) At C-band, both VV and VH are important for distinguishing forest types. The backscatter from acacia

in VV, but not VH, is greatly affected by whether peat or non-peat soils are present.
b) At L-band, HV carries most of the relevant information, and L-band is much more sensitive than C-band to structure arising from forest management. This can aid manually classification but is likely to induce errors in automatic classification. The backscatter from acacia is affected by whether the underlying soil is peat or non-peat for both HH and HV.
c) C-band time series allow plantation activity to be monitored and are likely also to be useful in detecting illegal forest clearance.

6. ACKNOWLEDGEMENT

This work was undertaken in part within the framework of the JAXA Kyoto and Carbon Initiative and also with data supplied by ESA.

7. REFERENCES

1. FAO. (2010). Global Forest Resource Assessment 2010. Rome: Food and Agriculture Organization of the United Nations.
2. DeFries, R. S., Rudel, T., Uriarte, M., & Hansen, M. C. (2010). Deforestation driven by urban population growth and agricultural trade in the twenty-first century. *Nature Geoscience,* **3**, 178-181.
3. Uryu, Y., Purastuti, E., Laumonier, Y., Budiman, A., Yulianto, K., Sudibyo, A., Stüwe, M. (2010). Sumatra's Forests, their Wildlife and the Climate. Windows in Time: 1985, 1990, 2000 and 2009. . Jakarta, Indonesia: WWF-Indonesia.
4. Susanti, A., & Burgers, P. (2012). Oil palm expansion in Riau Province, Indonesia: serving people, planet, profit. *Background paper for European Report on Development. Confronting scarcity: managing water, energy and land for inclusive and sustainable growth. Belgium: European Union*.
5. Uryu, Y., Mott, C., Foead, N., Yulianto, K., Budiman, A., Setiabudi, Stüwe, M. (2008). Deforestation, Forest Degradation, Biodiversity Loss and CO2 Emissions in Riau, Sumatra, Indonesia. WWF Indonesia Technical Report. Jakarta, Indonesia.
6. Jauhiainen, J., Hooijer, A., & Page, S. (2012). Carbon dioxide emissions from an Acacia plantation on peatland in Sumatra, Indonesia. *Biogeosciences*.
7. Fuller, D. O. (2006). Tropical forest monitoring and remote sensing: A new era of transparency in forest governance? *Singapore Journal of Tropical Geography* **27**, 15-29.
8. Hais, M., Jonášová, M., Langhammer, J., & Kučera, T. (2009). Comparison of two types of forest disturbance using multitemporal Landsat TM/ETM+ imagery and field vegetation data. *Remote Sensing of Environment,* **113**, 835–845.
9. Broich, M., Hansen, M. C., Potapov, P., Adusei, B., Lindquist, E., & Stehman, S. V. (2011). Time-series analysis of multi-resolution optical imagery for quantifying forest cover loss in Sumatra and Kalimantan, Indonesia. *International Journal of Applied Earth Observation and Geoinformation,* **13**(2), 277-291.
10. Dynamics, G. O. o. F. a. L. C. (2009). A sourcebook of methods and procedures for monitoring and reporting anthropogenic greenhouse gas emission and removals caused by deforestation, gains and losses of carbon stock in forests remaining forest, and forestation. *GOFC-GOLD Report Version COP15-1*.
11. Morton, D. C., DeFries, R. S., Shimabukuro, Y. E., Anderson, L. O., Del Bon Espírito-Santo, F., Hansen, M., & Carroll, M. (2005). Rapid assessment of annual deforestation in the Brazilian Amazon using MODIS data. *Earth Interactions,* **9**(8), 1-22.
12. Hansen, M. C., Shimabukuro, Y. E., Potapov, P. V., & Pitman, A. J. (2008). Comparing annual MODIS and PRODES forest cover change data for advancing monitoring of Brazilian forest cover. *Remote Sensing of Environment,* **112,** 3784-3793.
13. Sánchez-Azofeifa, G. A., Castro-Esau, K., Kurz, W., & Joyce, A. (2009). Monitoring carbon stocks in the tropics and the remote sensing operational limitations: from local to regional projects. *Ecological Applications,* **19**(2), 480-494.
14. Le Toan, T., Quegan, S., Davidson, M. W. J., Balzter, H., Paillou, P., Papathanassiou, K., Ulander, L. (2011). The BIOMASS mission: Mapping global forest biomass to better understand the terrestrial carbon cycle. *Remote Sensing of Environment,* **115**(11), 2850-2860.
15. Neumann, M., Ferro-Famil, L., & Reigber, A. (2010). Estimation of forest structure, ground, and canopy layer characteristics from multibaseline polarimetric interferometric SAR data. *Geoscience and Remote Sensing, IEEE Transactions on,* **48**(3), 1086-1104.
16. Whittle, M., Quegan, S., Uryu, Y., Stüewe, M., & Yulianto, K. (2012). Detection of tropical deforestation using ALOS-PALSAR: A Sumatran case study. *Remote Rensing of Environment,* **124**, 83-98.
17. Torres, R., Snoeij, P., Geudtner, D., Bibby, D., Davidson, M., Attema, E., Rostan, F. (2012). GMES Sentinel-1 mission. *Remote Sensing of Environment,* **120**, 9-24.
18. Shimada, M., & Ohtaki, T. (2010). Generating large-scale high-quality SAR mosaic datasets: Application to PALSAR data for global monitoring. *IEEE Journal of Selected Topics in Applied Earth Observations and Remote Sensing,* **3**(4), 637.
19. EnviSat ASAR product Handbook (2007). *European Space Agency*.
20. Quegan, S., & Yu, J. J. (2001). Filtering of

Multichannel SAR images. *IEEE Transactions on Geoscience and Remote Sensing*, **39**(11), 2373-2379.

21. JAXA, EORC. K&C Mosaic homepage, from http://www.eorc.jaxa.jp/ALOS/en/kc_mosaic/kc_mosaic.htm
22. Shimada, M., Isoguchi, O., Tadono, T., & Isono, K. (2009). PALSAR radiometric and geometric calibration. *Geoscience and Remote Sensing, IEEE Transactions on*, **47**(12), 3915-3932.
23. Oliver, C., & Quegan, S. (2004). *Understanding Synthetic Aperture Radar Images*. Raleigh: SciTech.